

# Measuring the fusion cross-section of $^{39,47}\text{K} + ^{28}\text{Si}$ at near-barrier energies

---

Justin Vadas, V. Singh, B. Wiggins, J. Huston, S. Hudan, R.T. de Souza; Indiana University Bloomington

A. Chbihi, D. Ackermann; GANIL

M. Famiano; Western Michigan University

K. Brown; Michigan State University



# Motivation: To understand the character of neutron-rich nuclear matter

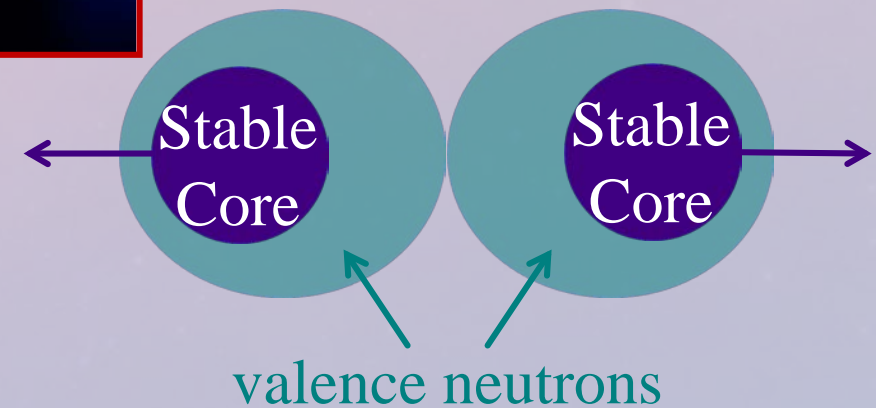
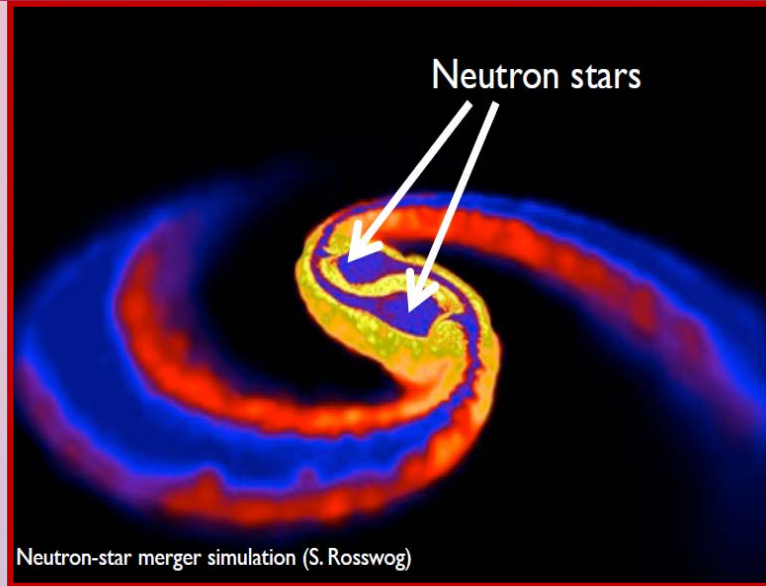
Understanding neutron-rich matter is important for a broad range of phenomena:

- Nucleosynthetic r-process
- Neutron star mergers

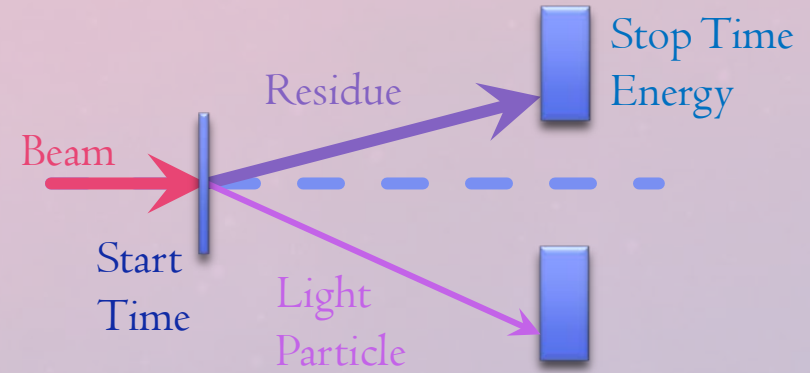
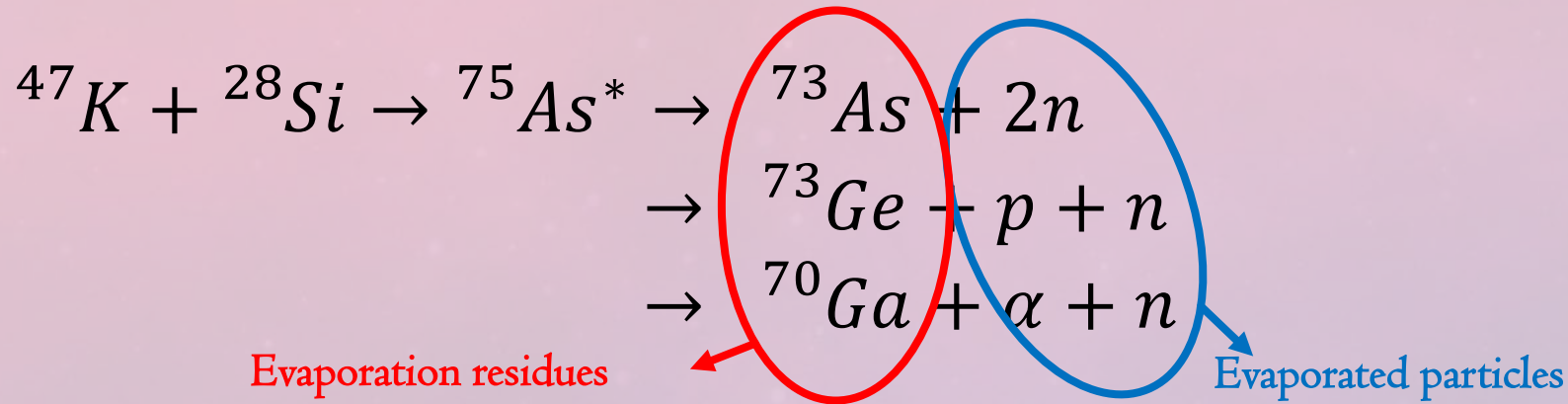
One laboratory to investigate the character of neutron rich matter is the skin of neutron-rich nuclei

The enhanced fusion of neutron-rich nuclei may serve to ignite X-ray superbursts in accreting neutron stars.

Gain insight into neutron skin by investigating fusion for an isotopic chain of neutron-rich nuclei (interplay of nuclear structure and dynamics)



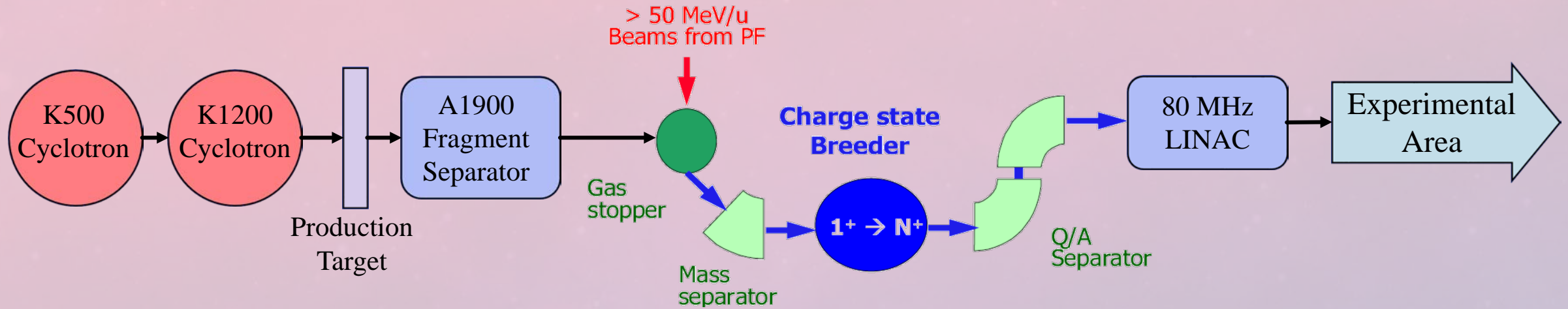
# The Reaction and its Products



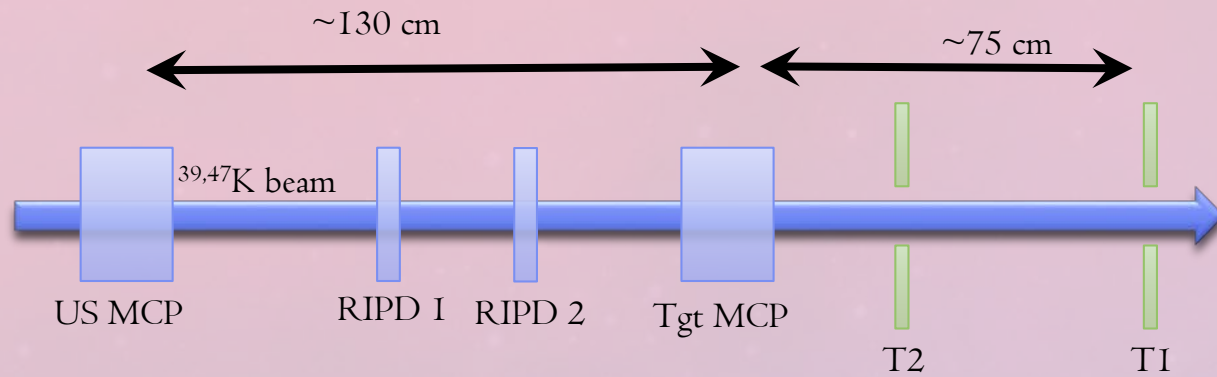
$$E = \frac{1}{2}mv^2 \quad m \propto Et^2$$

- Excited compound nucleus decays by emitting protons, neutrons, and particles
- The resulting heavy nucleus is known as an evaporation residue
- Emission of these light particles impart transverse momentum on the residue, kicking them off zero degrees and allowing for direct measurement of the residues and light particles

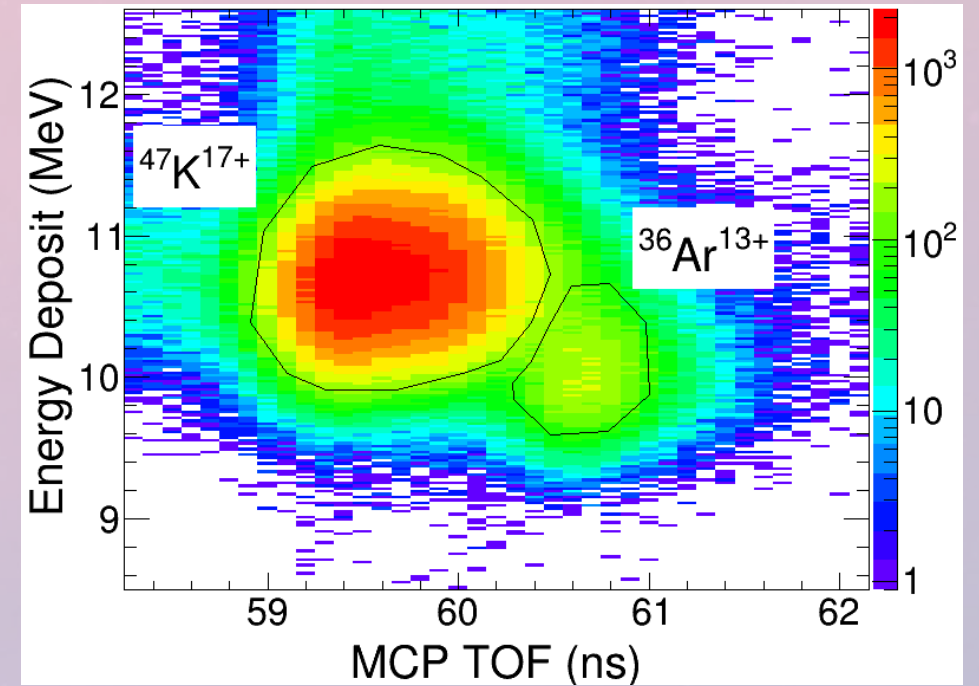
# Low energy rare isotope beams at NSCL



- Primary beam accelerated by two coupled cyclotrons
- Rare isotope beam (RIB) produced via projectile fragmentation and separated by A1900 spectrometer
- Beam significantly slowed down in a linear gas stopper
- Beam ionized to high  $N^+$  charge state in charge breeder
- RIB is re-accelerated to desired energy and delivered to the experimental area

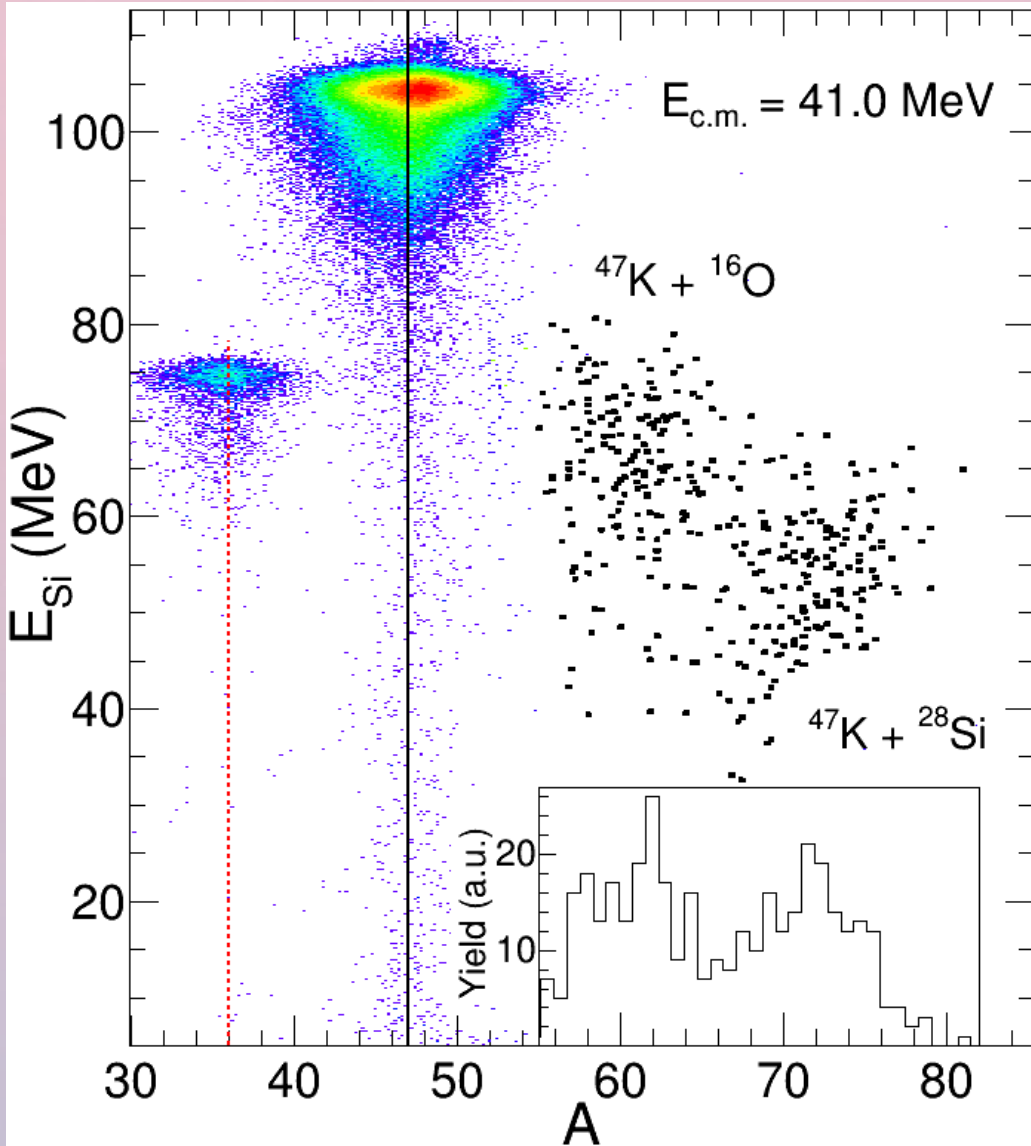


- $E_{\text{lab}} = 2.3 - 3 \text{ MeV/A}$
- Average intensity  $\sim 10^4 \text{ p/s}$
- Reaction products distinguished by ETOF
- Energy measured in segmented annular silicon detectors (T1, T2)  $1^\circ \leq \theta_{\text{lab}} \leq 7.3^\circ$
- Fusion product time-of-flight measured between target MCP and silicon detectors



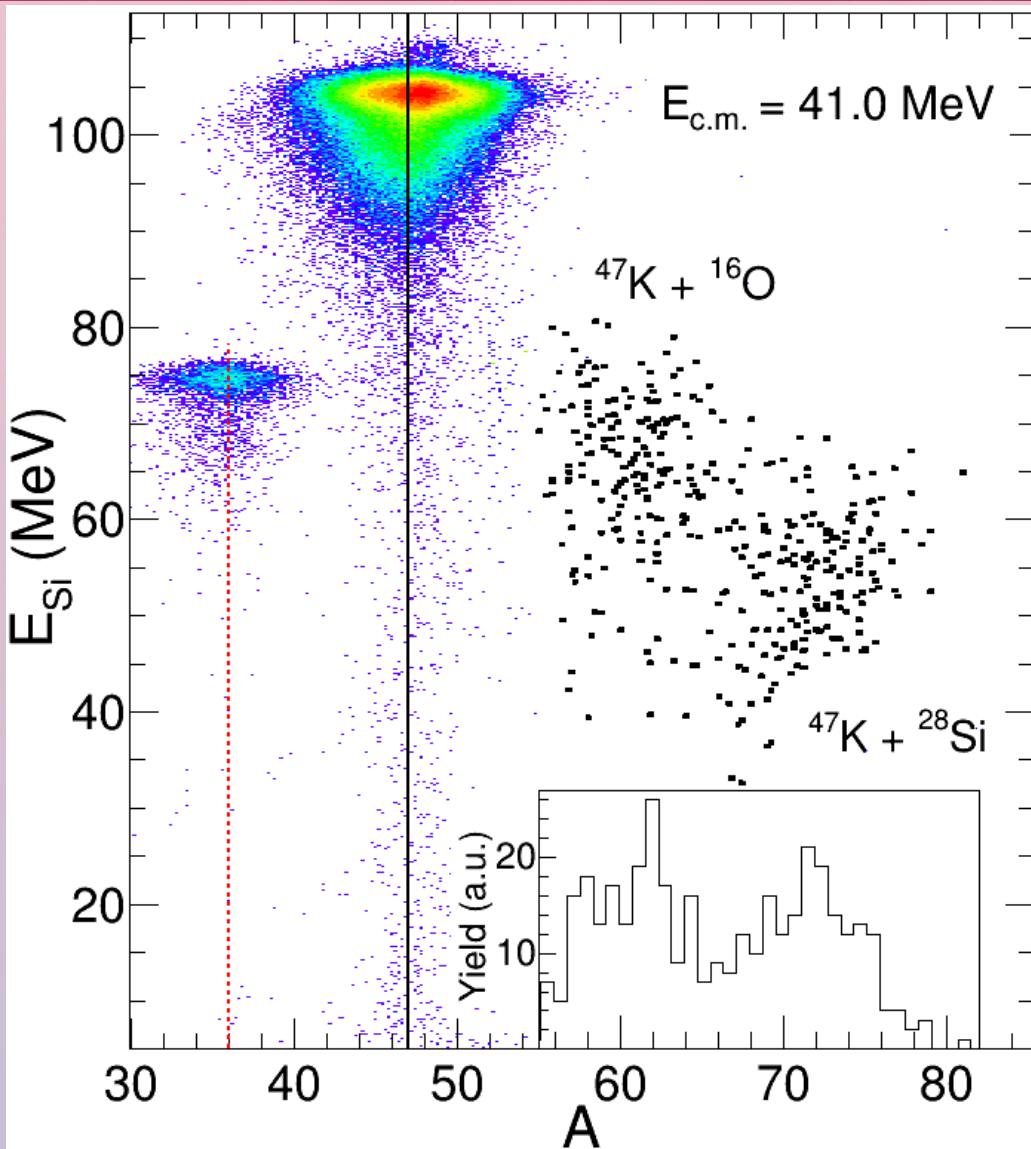
- ${}^{47}\text{K}$  beam contaminated by  ${}^{36}\text{Ar}$  ( $\sim 5\%$ )
- Particle identification performed using  $\Delta E$ -TOF
- $\Delta E$  measured in RIPD
- TOF measured between two MCP detectors

# Measuring evaporation residues



- Energy vs. time-of-flight linearized using the relation
$$A \propto Et^2$$
- Mass resolution  $\sim 2.4$  amu at  $A = 47$
- Clear separation is observed between evaporation residues and scattered beam
- Evaporation residues from two reactions:
  - $\text{K} + \text{O}$
  - $\text{K} + \text{Si}$
- ERs from each reaction are better separated by their mass-energy correlation in 2D

# Measuring evaporation residues

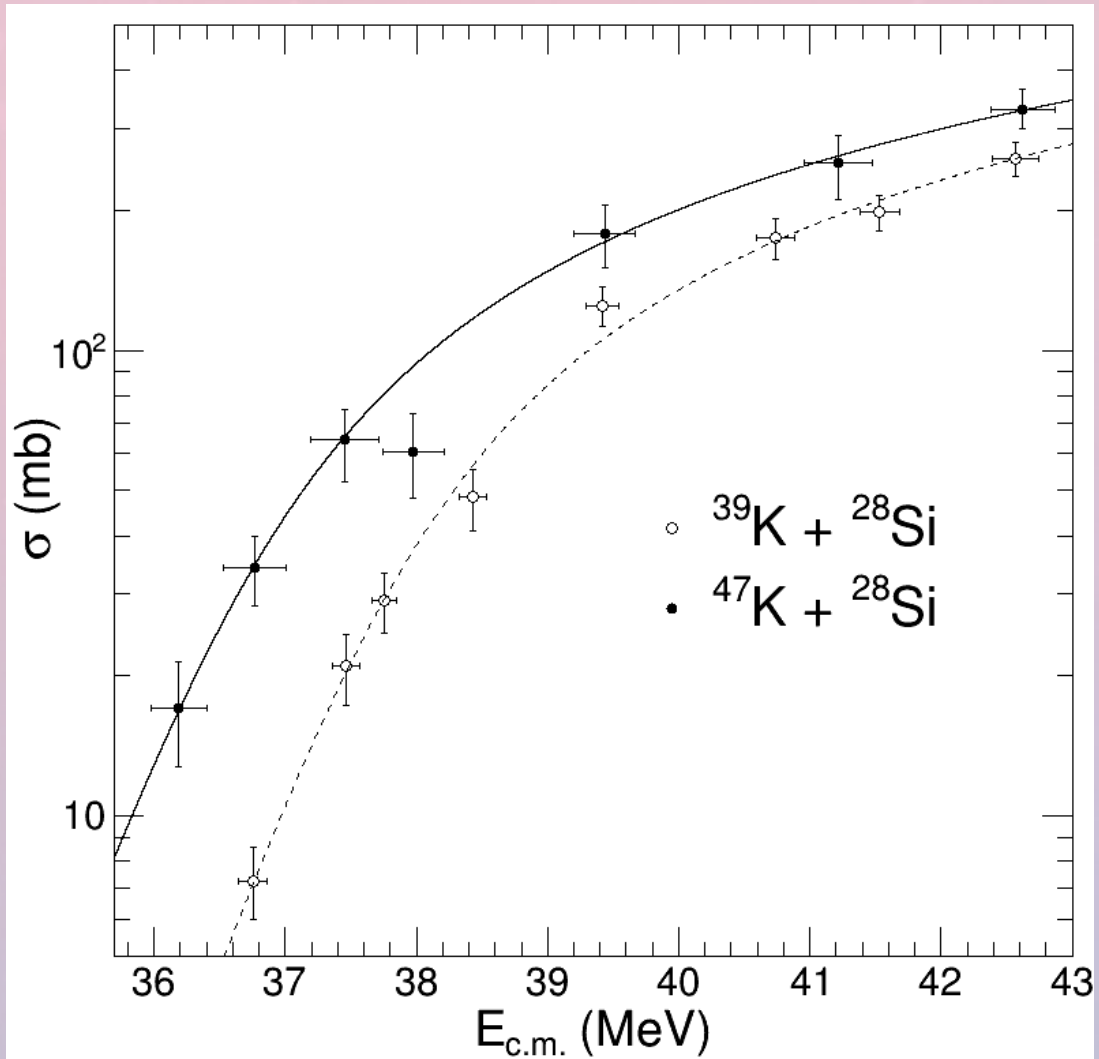


$$\sigma_{fusion} = \frac{N_{ER}}{N_{Beam} t \epsilon_{ER}}$$

Cross-section  $\rightarrow$   $\sigma_{fusion}$   $\leftarrow$  Number of residues  $N_{ER}$   
 $N_{Beam}$   $\leftarrow$  Beam count  $t$   $\leftarrow$  Target thickness  $\epsilon_{ER}$   $\leftarrow$  Efficiency

- Evaporation residues identified by mass are integrated ( $N_{ER}$ )
- The number of incident beam particles are counted with the two MCP timing detectors ( $N_{Beam}$ )
- Efficiency correction for detector geometric coverage ( $\epsilon_{ER}$ ) determined with statistical model (evapOR)
- Target thickness ( $t$ ) determined using the  $^{39}\text{K} + ^{16}\text{O}$  data and  $\alpha$  source energy loss measurements ( $^{241}\text{Am}$  and  $^{148}\text{Gd}$ )

# Fusion excitation function



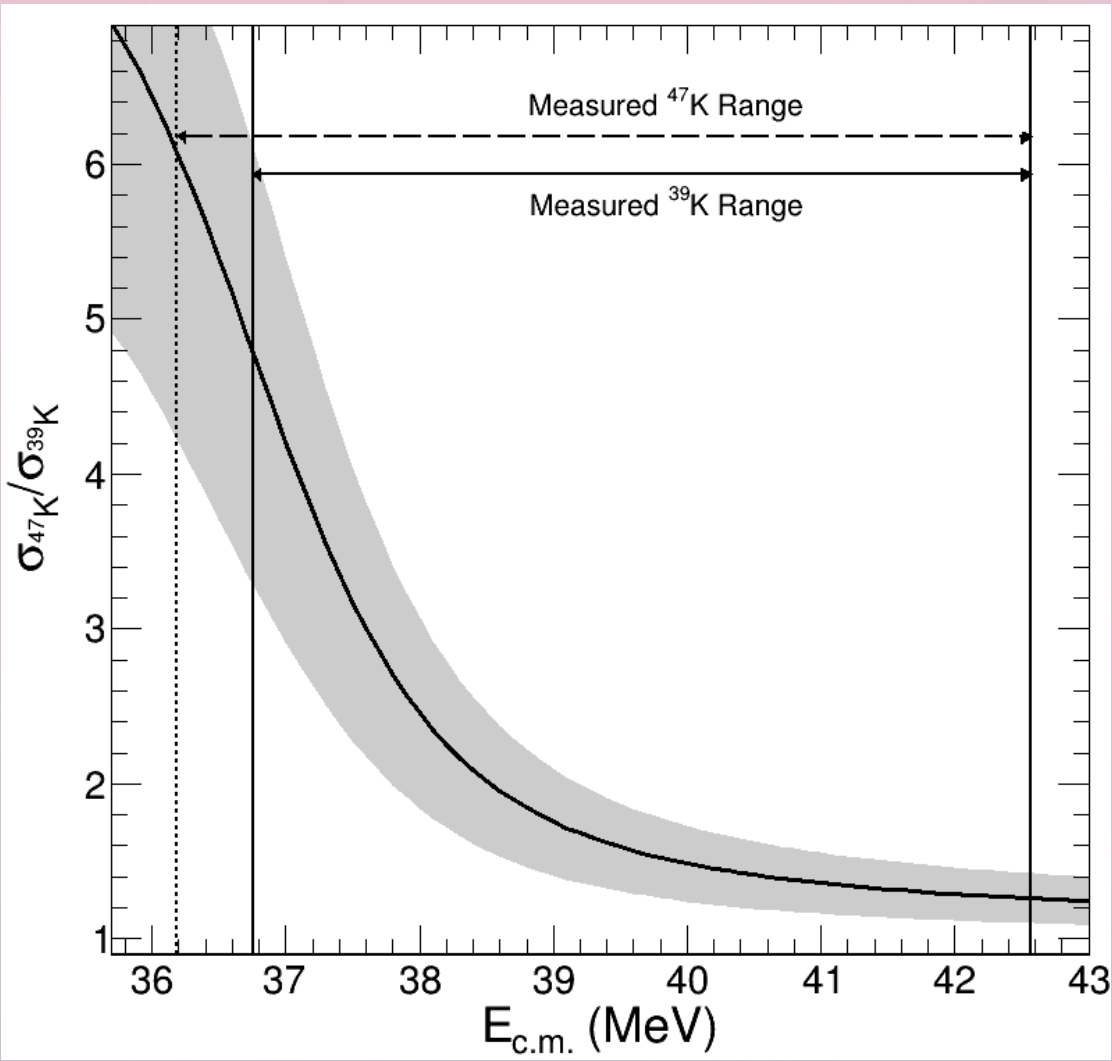
- First measurements of  $^{39,47}\text{K} + ^{28}\text{Si}$
- At all energies, the cross-section for  $^{47}\text{K}$  is higher than that for  $^{39}\text{K}$
- A one-dimensional parabolic barrier penetration formula (Wong formula) is used to parameterize the cross-sections

$$\sigma_{fusion} = \frac{R_c^2}{2E_{cm}} \hbar\omega \left\{ 1 + \exp \left[ \frac{2\pi}{\hbar\omega} (E_{cm} - V_c) \right] \right\}$$

- The relative cross-section can be used to facilitate better comparison between the two systems

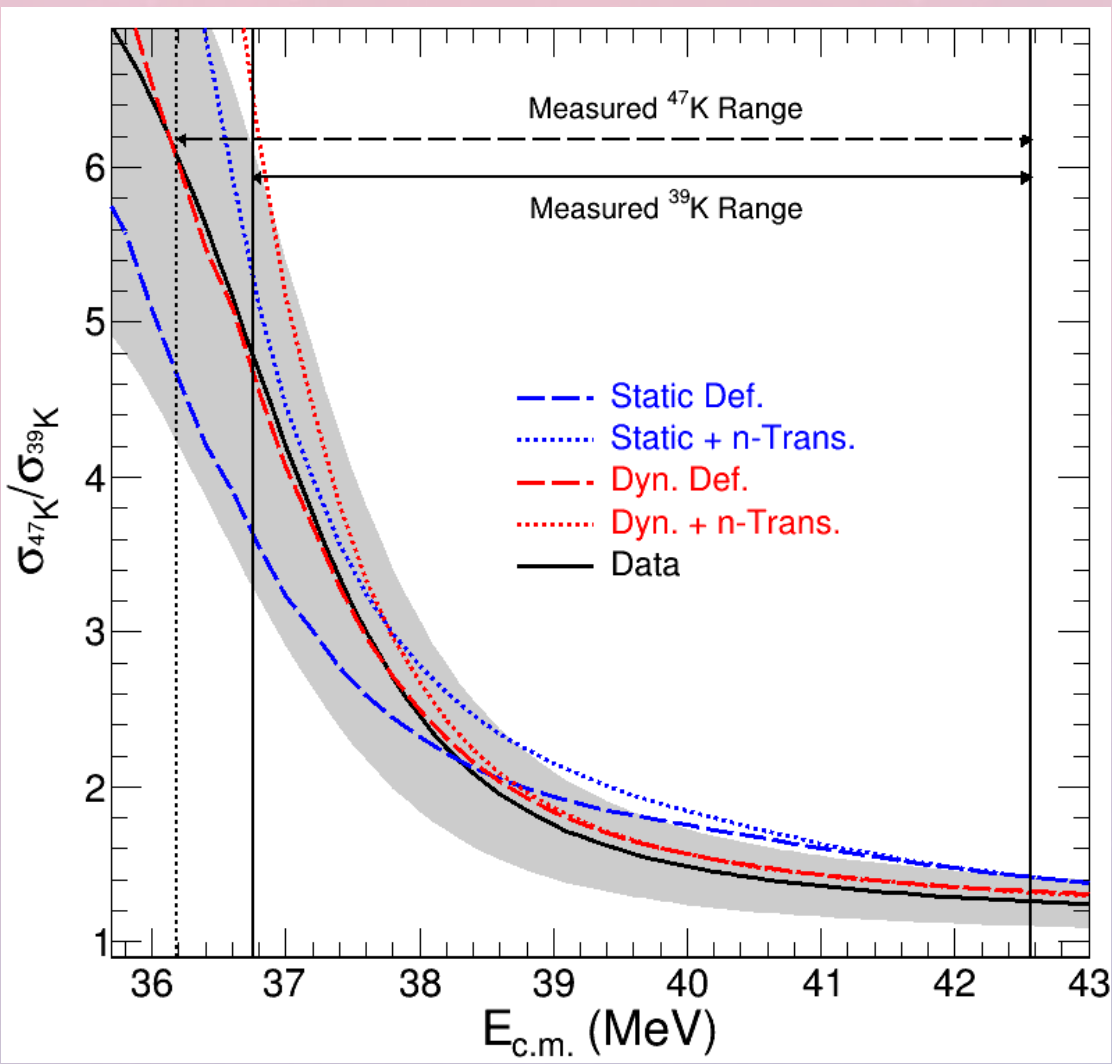


# Fusion excitation function



- As  $E_{\text{c.m.}}$  decreases and approaches the barrier, the cross-sections for  $^{47}\text{K}$  begin to drastically increase

# Fusion excitation function



- As  $E_{c.m.}$  decreases and approaches the barrier, the cross-sections for  $^{47}\text{K}$  begin to drastically increase
- Semi-empirical channel-coupling model code by Zagrebaev:
  - Initial statically deformed projectile and target
  - Allow projectile and target to deform on approach
  - Include the influence of neutron-transfer
- Observed enhancement can be described in the context of dynamic deformation of the projectile and target nuclei

<http://nrv.jinr.ru/nrv/>

V.I. Zagrebaev, Phys. Rev. C 64 (2001) 034606

V.I. Zagrebaev, et al., Phys.Rev. C 65 (2002) 014607

# Conclusions/Outlook

## Summary

- The fusion cross-section for  $^{39,47}\text{K} + ^{28}\text{Si}$  has been measured for the first time using the ReA3 facility at NSCL
- A significant enhancement of the cross-section (up to a factor of 6) is observed for  $^{47}\text{K}$  relative to  $^{39}\text{K}$  near the barrier
- This enhancement can be understood as dynamic deformation of the system as the projectile and target approach

## In the future:

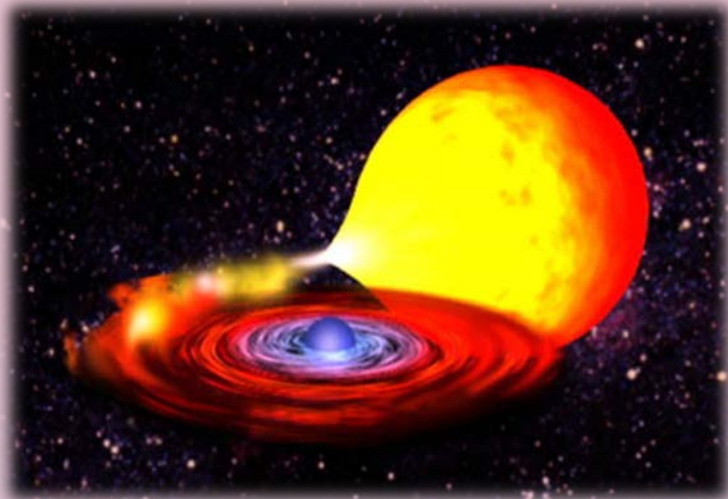
- Compare cross-sections with other models such as DC-TDHF and CCFULL
- $^{41,45}\text{K} + ^{28}\text{Si}$  and  $^{36,44}\text{Ar} + ^{28}\text{Si}$  at NSCL ReA3 (E17002)
- $^{20,21}\text{O} + ^{12}\text{C}$  at GANIL (E739), possibly  $^{22}\text{O}$  (LOI)

# Acknowledgements

- Indiana University:
  - Nuclear Chemistry group
  - IU Mechanical Instrument Services
  - IU Electronic Instrument Services
- GANIL:
  - Abdou Chbihi, Dieter Ackermann
- Western Michigan University:
  - Mike Famiano, Mike Bischak
- Michigan State University:
  - Kyle Brown, Clementine Santamaria
  - Technical staff at NSCL/ReA3
    - Antonio Villari, Sam Nash, Alain LaPierre

# Additional Material

# X-ray superbursts

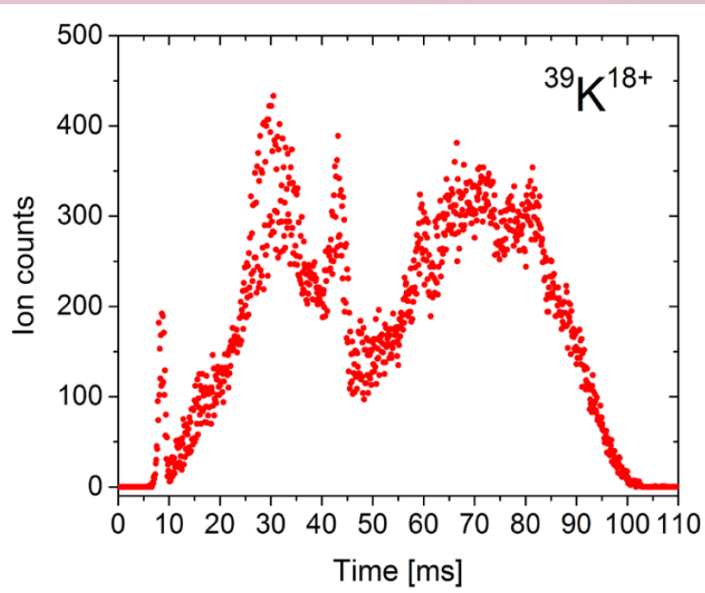


		$^{38}\text{Ca}$ 440 ms	$^{39}\text{Ca}$ 860 ms	$^{40}\text{Ca}$ 3e21 y	$^{41}\text{Ca}$ 1e5 y	$^{42}\text{Ca}$ stable	$^{43}\text{Ca}$ stable	$^{44}\text{Ca}$ stable	$^{45}\text{Ca}$ 162.6 d	$^{46}\text{Ca}$ 3e17 y	$^{47}\text{Ca}$ 4.54 d	$^{48}\text{Ca}$ 6e22 y	$^{49}\text{Ca}$ 8.72 m
Z	20	$^{37}\text{K}$ 1.226 s	$^{38}\text{K}$ 7.636 m	$^{39}\text{K}$ stable	$^{40}\text{K}$ 1e9 y	$^{41}\text{K}$ stable	$^{42}\text{K}$ 12.3 hr	$^{43}\text{K}$ 22.3 hr	$^{44}\text{K}$ 22.1 m	$^{45}\text{K}$ 17.8 m	$^{46}\text{K}$ 105 s	$^{47}\text{K}$ 17.5 s	$^{48}\text{K}$ 6.8 s
	19	$^{36}\text{Ar}$ stable	$^{37}\text{Ar}$ 35.04 d	$^{38}\text{Ar}$ stable	$^{39}\text{Ar}$ 269 y	$^{40}\text{Ar}$ stable	$^{41}\text{Ar}$ 109 m	$^{42}\text{Ar}$ 32.9 y	$^{43}\text{Ar}$ 5.37 m	$^{44}\text{Ar}$ 11.9 m	$^{45}\text{Ar}$ 21.5 s	$^{46}\text{Ar}$ 8.4 s	$^{47}\text{Ar}$ 1.23 s
	18	18	19	20	21	22	23	24	25	26	27	28	29
		N											

- An X-ray superburst, which occurs in the outer crust of an accreting neutron star, releases more energy in a few hours than the sun does in a decade
- Fusion of light and mid-mass neutron-rich nuclei has been proposed as being responsible for triggering X-ray superbursts
- Measurement of an isotopic chain provides information on how structure and dynamics evolve with increasing neutron number
- $^{39,47}\text{K} + ^{28}\text{Si}$  allows for exploring the effect of a large span in neutron number on fusion

# Challenges experienced with ReA3

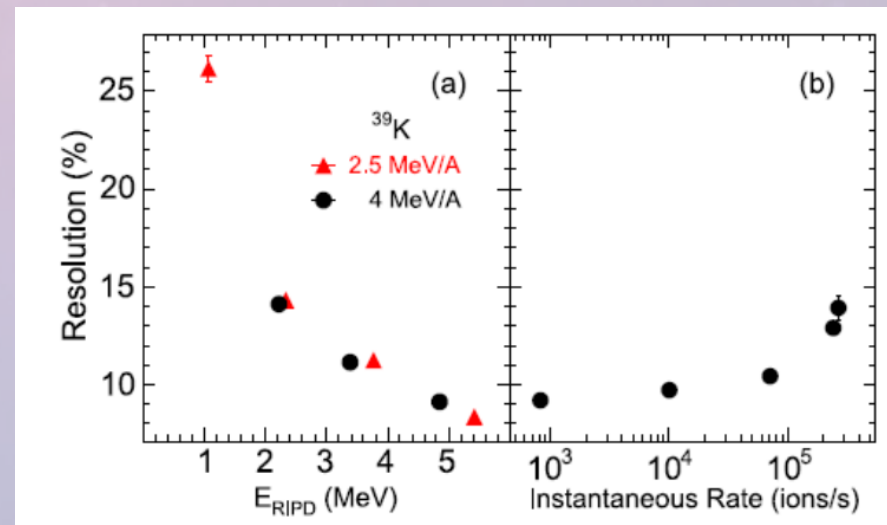
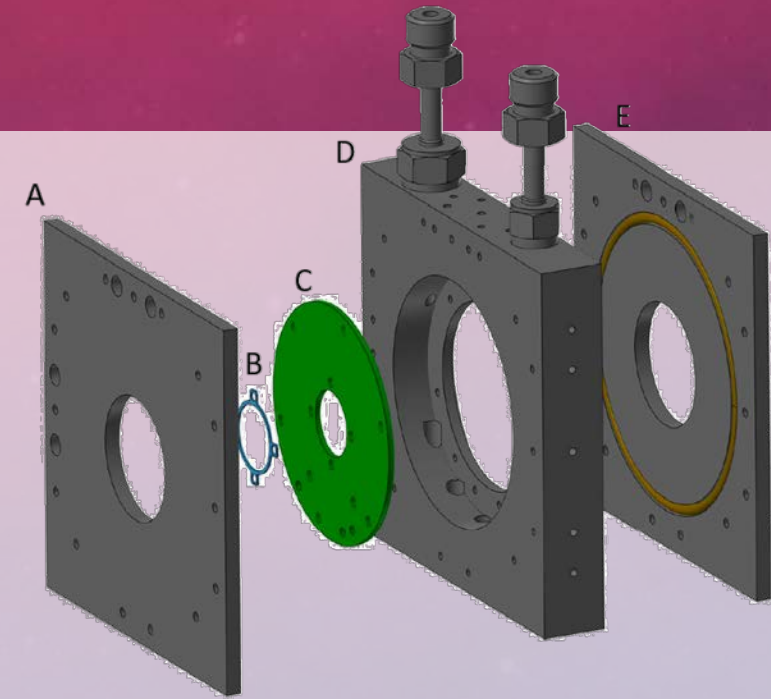
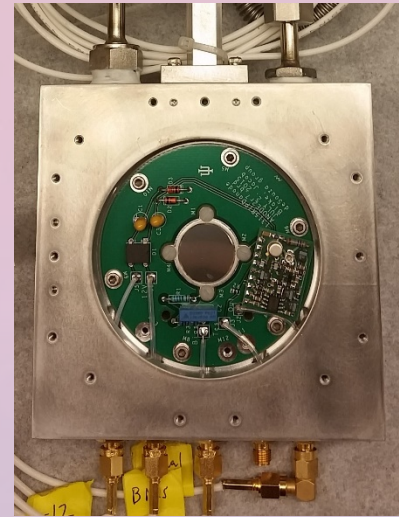
- Timing structure of the beam
  - Beam leaves the charge breeder in macrobursts every 500 ms (2 Hz)
  - The ions are bunched into the first  $\sim 100$  ms of each macroburst
  - Instantaneous rate experienced by detectors:  $\sim 5x$  higher than the average rate
- Contamination in RIBs
  - Particle identification is required on an event-by-event basis
  - Need detector with good energy resolution and high rate capability



# Rare Ion Purity Detector (RIPD)

- Axial field design with central anode minimizes charge collection time
- Aluminized windows serve as cathodes ( $0.5 \mu\text{m}$ )
- Utilize  $\text{CF}_4$  as detector gas based upon its high electron drift velocity
- Integrated fast charge sensitive amplifier
- Energy resolution  $\sim 8\%$  above 5 MeV
- Resolution  $\sim 10\%$  at an instantaneous rate of  $1 \times 10^5$  ions/s

J. Vadas, *et al.*, NIMA 837 (2016) 28

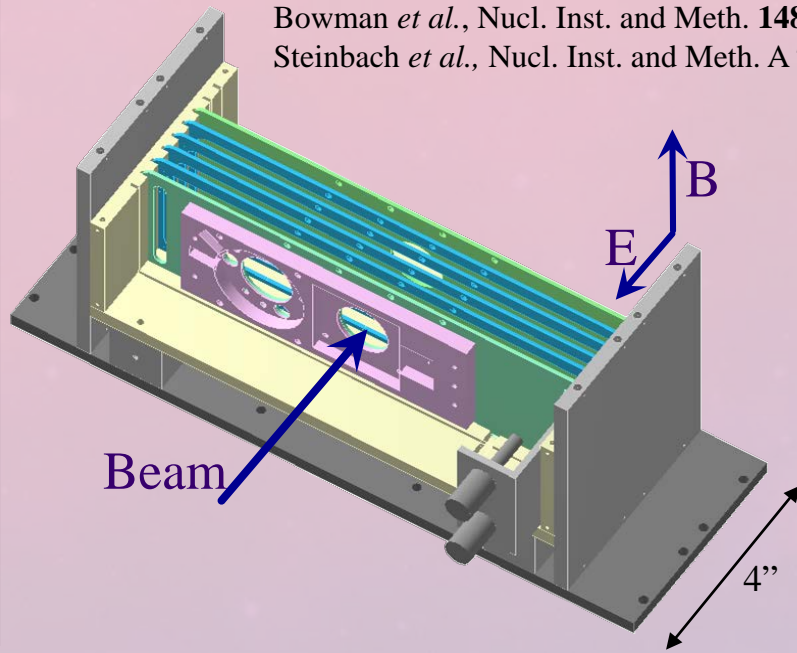


A: Window plate  
B: Anode foil ring  
C: PCB for charge sensitive amplifier  
D: Detector body  
E: Window plate



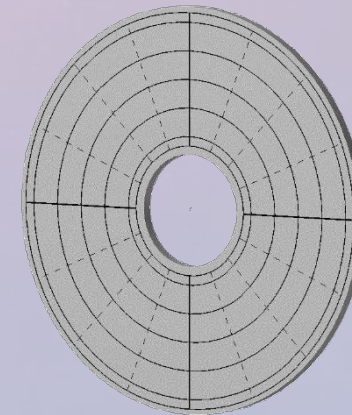


Bowman *et al.*, Nucl. Inst. and Meth. **148**, 503 (1978)  
 Steinbach *et al.*, Nucl. Inst. and Meth. A **743**, 5 (2014)



- E x B fields transport electrons from secondary emission foil to MCP
- E field produced by biasing array of ring plates
- B field produced by NdFeB permanent magnets
- Timing resolution  $\sim 300$  ps

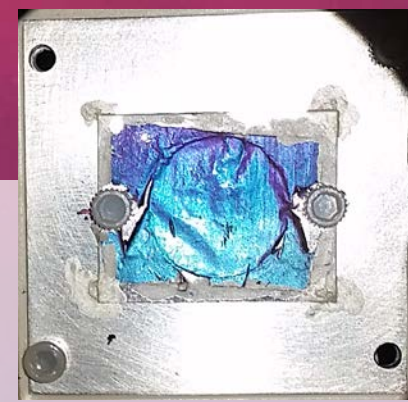
- Annular single crystal Si(IP) detectors
- Segmented to provide angular information and reduce detector capacitance
- Timing resolution  $\sim 450$  ps
- Energy resolution  $< 1\%$



deSouza *et al.*, Nucl. Instr. and Meth. **A632**, 133 (2011)

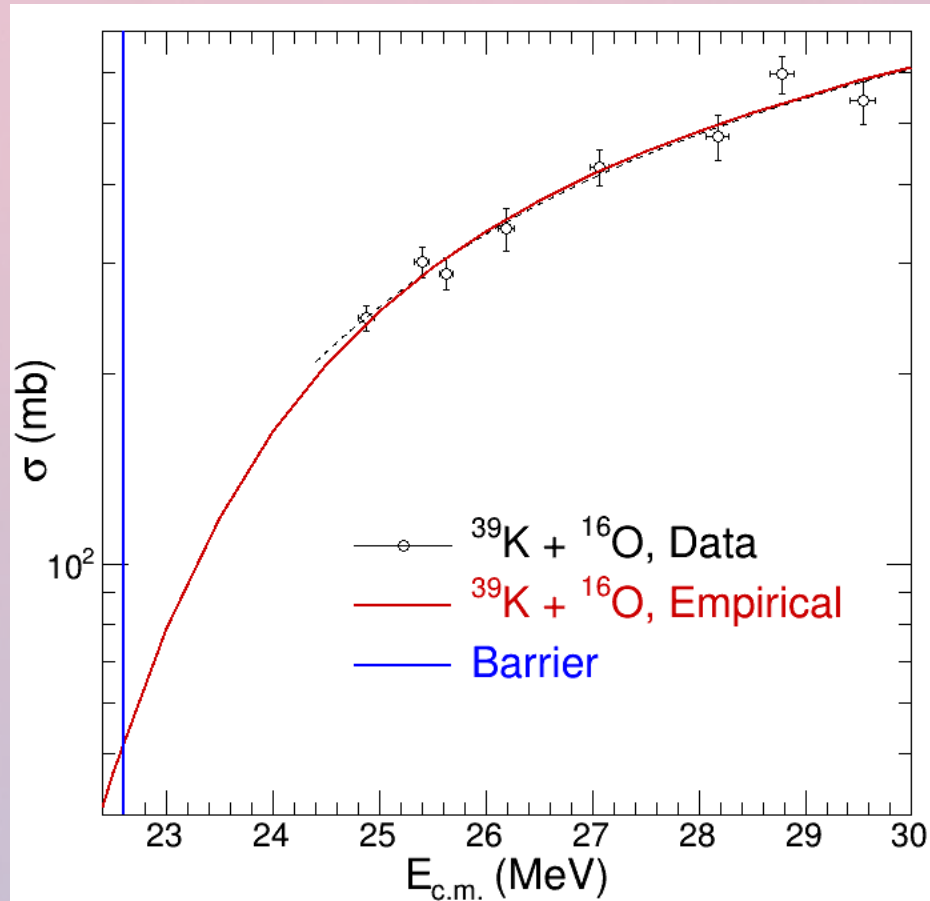
# Determining the target thickness

$^{28}\text{Si}$  enriched target provided by M. Loriggiola (Legnaro National Laboratory)



Estimating the amount of oxidation:

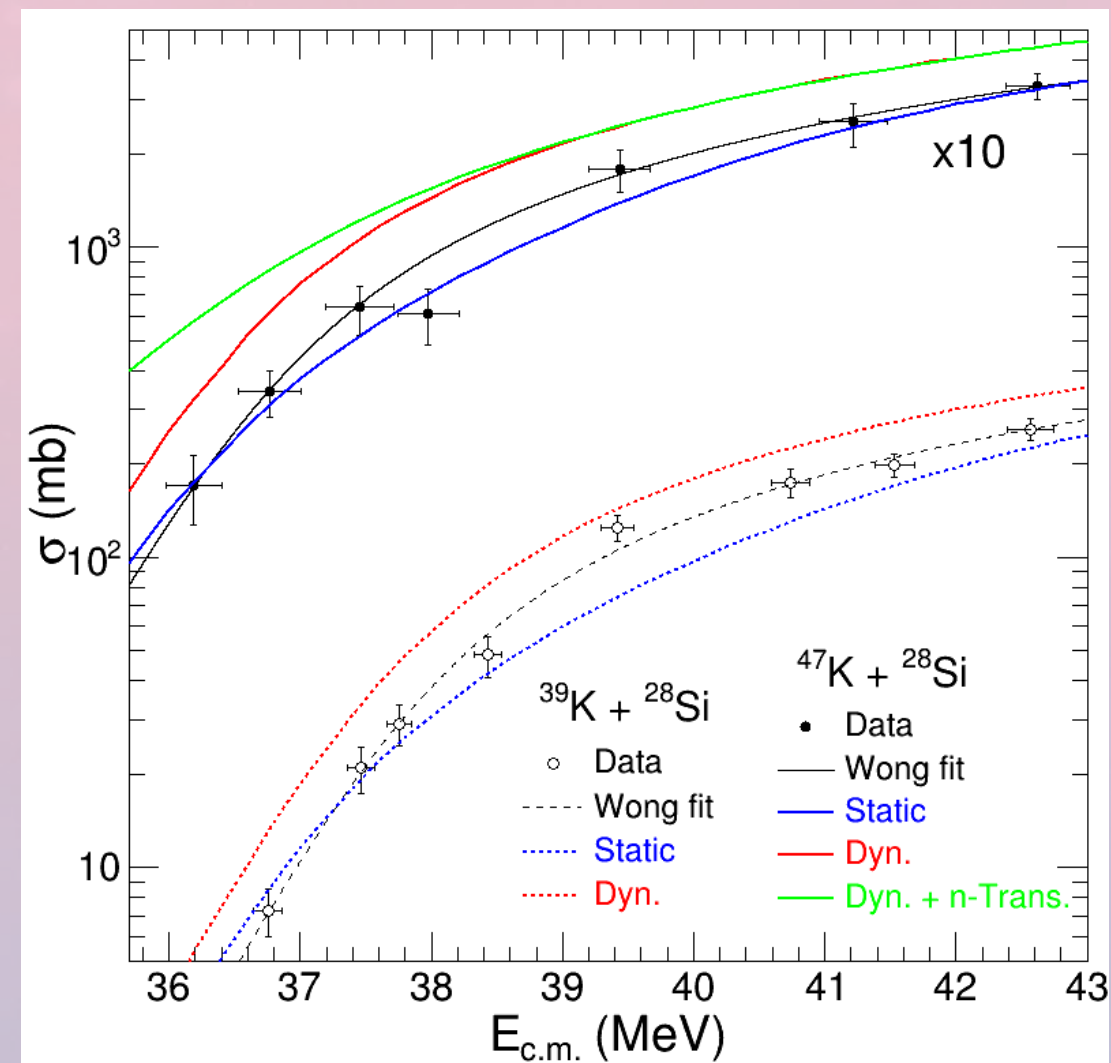
- Extracted  $\frac{\sigma_{fusion}}{t_{^{16}\text{O}}}$  for  $^{39}\text{K} + ^{16}\text{O}$
- Calculated  $\sigma_{fusion}$  from empirical channel coupling model
- Minimized  $\chi^2$  in calculating  $t$  for  $^{16}\text{O}$
- $t_{^{16}\text{O}} \rightarrow t_{\text{SiO}_2}$
- $t_{^{16}\text{O}} = 97 \mu\text{g}/\text{cm}^2$ ;  $t_{\text{SiO}_2} \approx 800 \text{ nm}$



Determining the amount of  $^{28}\text{Si}$ :

- Measured energy loss of  $\alpha$  particles from  $^{148}\text{Gd}$  and  $^{241}\text{Am}$  sources
- Using SRIM and known  $t_{\text{SiO}_2}$ , determined  $t_{^{28}\text{Si}_{\text{pure}}}$
- Total thickness =  $327 \mu\text{g}/\text{cm}^2$   $^{28}\text{Si}$

# Fusion excitation function



- Static deformation results in a too-shallow excitation function for both systems
- Dynamic deformation has the same shape as the data, but is systematically higher for all energies for both systems
- Inclusion of neutron-transfer channels only influences the cross-sections at below-barrier energies for  $^{47}\text{K}$